

SYNTHESIS AND CHARACTERIZATION OF PURE AND NI DOPED TITANIA NANORODS FOR ENHANCED VISIBLE LIGHT PHOTOCATALYTIC ACTIVITY

G. NAGARAJ, Dr. A. Dhayal Raj, Dr. A. Albert Irudayaraj

¹Research scholar, SHC-Tirupattur, ²Assistant Professor, SHC-Tirupattur

³Associate Professor, SHC-Tirupattur

Department of Physics

Sacred Heart College, Tirupattur, Vellore District, Tamilnadu, India-635601.

Abstract: Doping metal catalyst into TiO_2 matrix have very often improved the exciting properties of TiO_2 . Herein, Ni has been doped into TiO_2 and the effect of doping has been investigated. The properties of the prepared Ni doped and pure TiO_2 samples have been investigated via, XRD, SEM, HRTEM, EDAX and FTIR. XRD results confirm an increase in grain size on doping Ni. However it is also revealed that on increasing the calcination temperature, the grain size of Ni doped sample decreases. Ni doping has enhanced the growth of particles and this is confirmed through HRSEM and HRTEM results. The effect of doping Ni on the photocatalytic performance of TiO_2 has been investigated through Methylene Blue (MB) degradation under solar light. The results are impressive as Ni doped TiO_2 degrades MB with 30 min. Thus on doping Ni into TiO_2 matrix both the physical and chemical properties of the sample can be tailored accordingly.

Keyword: Pure Titania, Ni doped Titania, Solar light, Photocatalytic activity, HRTEM.

1. Introduction

The dye stuff lost in textile, plastic and leather industries poses a major problem to wastewater sources [1]. The world of photocatalyst projects TiO_2 as one of the best material because of its chemical stability, non-toxicity and low-cost. TiO_2 crystallites exist in three different structures: brookite, rutile and anatase. These three phases can be generally described as constitute by deal of the same building block- $Ti-O_6$ octahedron in which Ti atom is surrounded by six oxygen atoms situated at the corners. In spite of the similarities in building blocks of $Ti-O_6$ octahedral for these polymorphs, the electronic structures are significantly different. Among them, the anatase phase has the highest photocatalytic activity compared with the rutile and brookite phase [2-4]. However, the performance of the TiO_2 photocatalyst depends on its size, crystallinity, phase ratio, purity, etc. Amongst all these properties, size dependent property of semiconductor nanoparticles is unique. Titanium dioxide is the most active photocatalyst and commonly used in organic compound degradation. The widespread technological use of TiO_2 is impaired by its wide band gap, the fast charge-carrier recombination, and the low interfacial charge-transfer rates [5-8]. It offers a typical opportunity to fabricate new exotic devices of unprecedented nature.

Anatase has a near to the ground electron hole recombination rate and due to its high photoactivity is thought to be the most favorable phase for solar energy conversion and photocatalysis [9,10]. It is an n-type semiconductor among an indirect bandgap of 3.2 eV [11,12]. Particle size has great influence on the structure and properties of TiO_2 . In the nanometric organization, anatase is the most of stable polymorph [13-15]. However, but its full potential application was hampered by its activation only under ultraviolet light irradiation [16-17]. Therefore, current research has sought to improve the photocatalytic properties of TiO_2 . Doping with metals, oxides ions and precursor modification H_2O_2 have been demonstrated to be same effective routes to extend the absorption of TiO_2 to visible light region [18-21]. Among the metal dopants, Ni is one of the appropriate extensions of visible light photocatalytic activity of TiO_2 . Though various methods have been developed for the preparation of Ni doped TiO_2 , some of them involve expensive equipment or complicated steps.

Prasetyo Hermawan et.al., Siti Nur Fadhilah Zainudin et.al.,[22,23] they found that the presence of suitable amount of Ni into TiO_2 could improve the surface texture and enhance the thermal stability, crystal stability and high visible light utilizing. In the present work, we propose a novel and simple Photon Induced Method (PIM) for the preparation of Ni doped TiO_2 nanorods and pure TiO_2 nanoparticles. The effect of doping Ni into TiO_2 matrix has been analyzed and reported. We have also used these nanorods and nanoparticles as photocatalysts to study the photodegradation of Methylene blue under solar light for enhanced photocatalytic activity.

2. Experimental

2.1 Synthesis of the samples. Pure and Ni doped TiO_2 were synthesized through Photon Induced Method. All chemicals used are of analytic grade and are used without further purification. Titanium tetra isopropoxide (0.009 moles) and nickel nitrate (0.003 moles) are the starting materials. $Ti(OPr)_4$ and $Ni(NO_3)_4$ are mixed in double distilled water (500ml) and the solution is stirred for 7 hrs under the irradiation of halogen light (250W) and then the solution is left undisturbed in the dark for the remaining 17 hrs. The same procedure is followed for 3 days. After 3rd

day, the solution is kept in the open space for 3 more days. After which 200ml of double distilled water is added to the above solution and stirred for 1 hr with irradiation of halogen light. Then ammonia solution is added drop by drop until the pH of the solution reached 12. The stirring is continued for another 6 hrs and then solution was left undisturbed in the dark for remaining 17 hrs. Finally, the solution is exposed to Halogen light. The necessary precautions are taken not to disturb the setup for 7 hrs. Thus totally 8 days are taken for the synthesis of Ni doped TiO₂ by this method. The same procedure and reaction time is adopted for preparing pure TiO₂ nanoparticles with respect to synthesis. Ni doped TiO₂ and pure TiO₂ powder obtained finally are collected, washed, dried and calcinated for 1hr at required temperatures.

2.2. Characterization Studies

X-ray powder diffraction (XRD) pattern of the prepared sample were recorded on a Bruke D8 Advance powder X-ray diffractometer with Cu-K α ($\lambda = 1.5406 \text{ \AA}$). Particle size and morphology were ascertained via (FEI Quanta FEG 200) high resolution scanning electron microscope. High-resolution transmission electron microscopy (HRTEM) was done with transmission electron microscope JEOL 300 kV. EDAX measurements were carried out using instrument AMETEX. Perkin Elmer FTIR spectrometer, UV-via spectrometer Varian Cary Bio 50.

3. Results and Discussion

XRD patterns in figure 1a corresponding to pure TiO₂ nanoparticles calcinated at 500°C shows only anatase phase whereas figure 1b shows XRD pattern of Ni doped powder TiO₂ calcinated at 500°C, having rutile and anatase phase. However, traces of Ni element are not detected due to its low concentration. Figure 1(c and d) corresponds to the XRD pattern of pure and Ni doped samples calcinated at 900°C. Both the samples show a mixed phase of rutile and anatase. As the calcinations temperature is increased, the transformation of the phase favoring rutile is witnessed. Also, the doping of Ni into TiO₂ matrix favors the formation of rutile phase TiO₂. The grain size calculated with the help of Debye Scherrer formula suggest an increase in grain size from 5 nm to 26 nm when the calcination temperature of pure TiO₂ sample is increased from 500°C to 900°C. However an opposite behavior is witnessed in the Ni doped samples i.e the grain sizes of Ni doped sample calcinated at 500°C and 900°C are found to be 36 nm and 20 nm respectively. This decrease in the grain size may be correlated to the breaking and deformation up of nanorods [24, 25]. The decrease in grain size is again confirmed through the decrease in peak intensity of (101) plane (fig.1b and d).

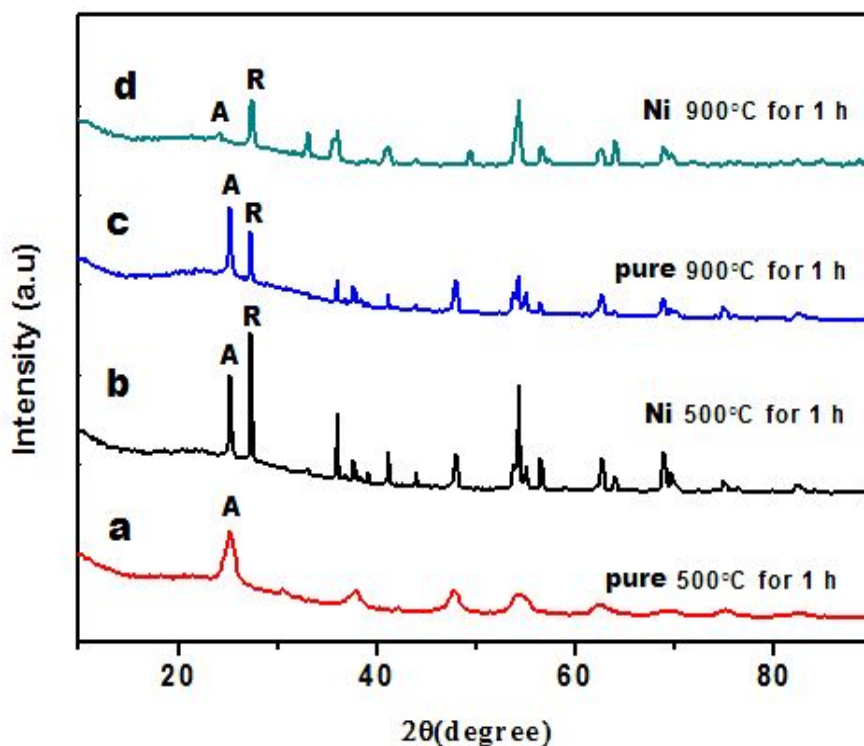


Figure 1 XRD pattern a)Pure TiO₂ calcinated 500°C, b)Ni doped TiO₂ calcinated 500°C, c) Pure TiO₂ calcinated 900°C, d) Ni doped TiO₂ calcinated 900°C

The surface morphology of pure TiO₂ and Ni doped TiO₂ have been studied using high resolution scanning electron microscope. Figure 2a shows the HRSEM image of pure TiO₂ nanoparticles in spherical shape with uniform size distribution. But, on doping Ni multi sized nanorods and spherical particles are witnessed with non uniform distribution as shown in figure 2b. This result is in accordance with the fact that Ni doping can alter the TiO₂ particles growth. Figure 3 shows the HRTEM micrographs of pure TiO₂ nanoparticles. Figure 3(a and b) correspond to the lower and higher magnification HRTEM micrographs of pure TiO₂ nanoparticles. Spherical nanoparticle with lot of agglomeration is seen. However the approximate particle size is found to be in the range of 40-60 nm. The lower and higher magnification HRTEM images in figure 3(c and d) correspond to the Ni doped TiO₂ samples. Figure 3c shows a mixture of nanoparticles and nanorods. The dimension of the nanorod as obtained

from figure 3d is 35 nm width and 85 nm length. Figure 4 shows the EDAX spectrum of pure and Ni doped TiO₂. The spectrum shows the chemical constituents of Ti, O and Ni present in the samples

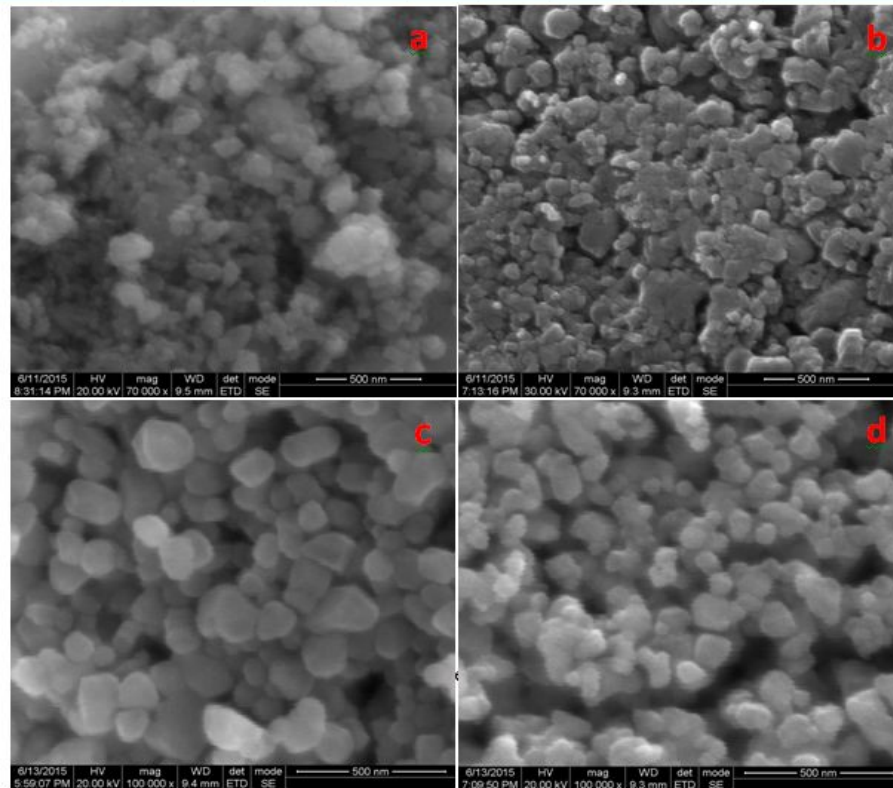


Figure 2 HRSEM image of a) Pure TiO₂ calcinated at 500°C, b) Pure TiO₂ calcinated at 900°C, c) Ni doped TiO₂ calcinated at 500°C and d) Ni doped TiO₂ calcinated at 900°C

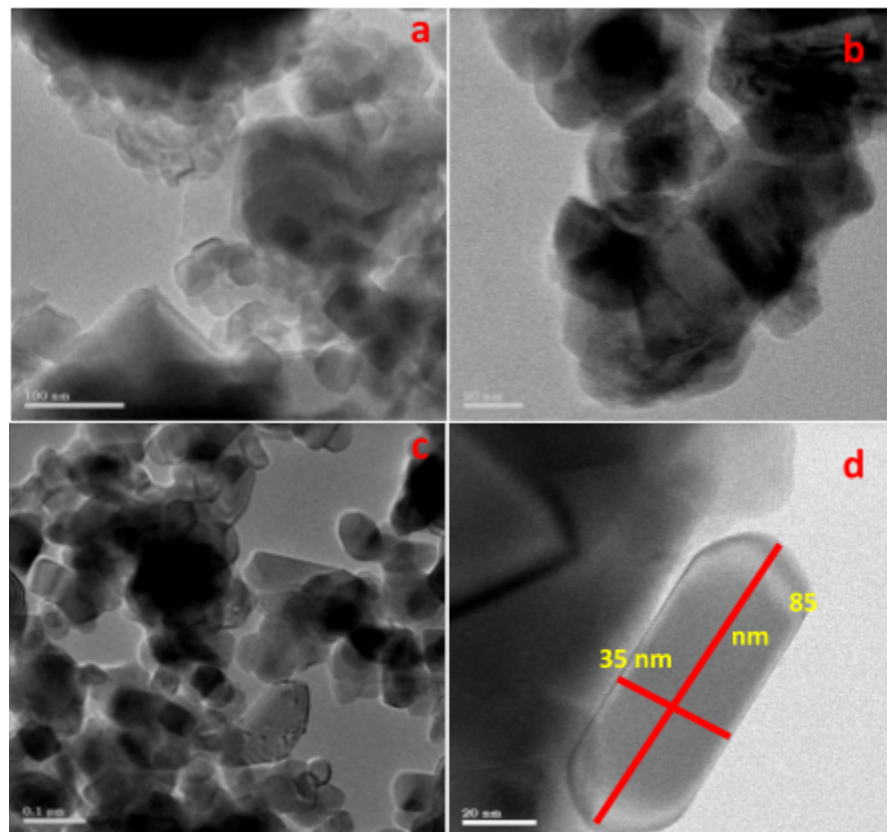


Figure 3 HRTEM show in (a and b) lower and higher magnification image of pure TiO₂ calcinated at 900°C and (c and d) lower and higher magnification image of Ni doped TiO₂ calcinated at 900°C

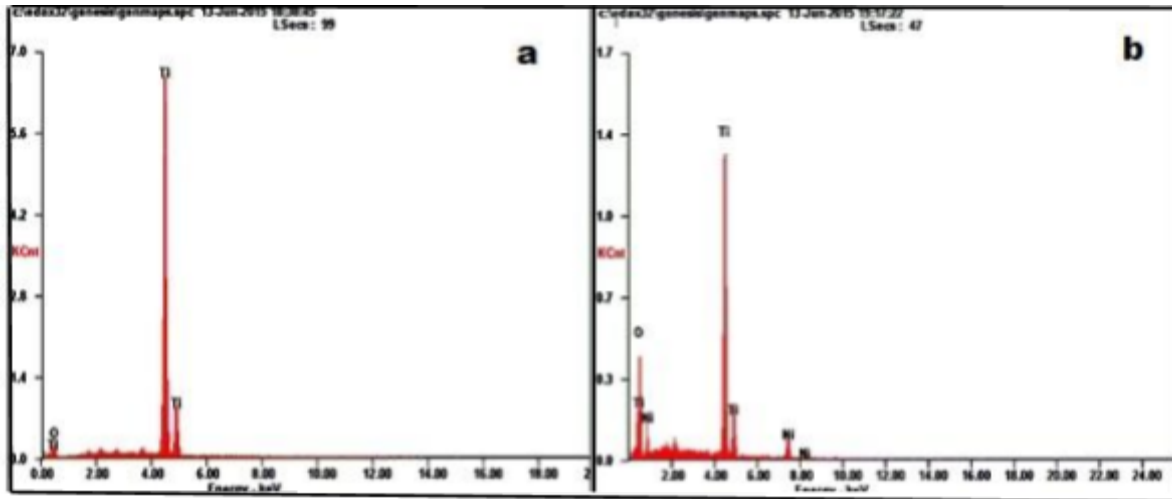


Figure 4 EDAX a) pure TiO_2 calcinated at 900°C b) Ni doped TiO_2 calcinated at 900°C

The presence of Ni confirms the doping of Ni in TiO_2 matrix. The FTIR spectrum of pure and Nickel doped TiO_2 nanoparticles are shown in figure 5 (a and b). The broadband spectrum occurring at $530\text{--}750\text{ cm}^{-1}$ correspond to metal oxides [26, 27]. This may be attributed to the Ti-O bending vibration and shows the formation of metal oxide bonding in the prepared sample. Whereas, the characteristic peaks at 1619 cm^{-1} and 3962 cm^{-1} are associated with the O-H bending vibration of the water molecules absorbed on TiO_2 surfaces in pure TiO_2 and Ni doped TiO_2 [28,29]. Also the peaks obtained at 3420 cm^{-1} is due to stretching vibration of O-H groups in the samples surface [30]. The adsorption of water from moisture during sample preparation has been reported earlier [31 -33].

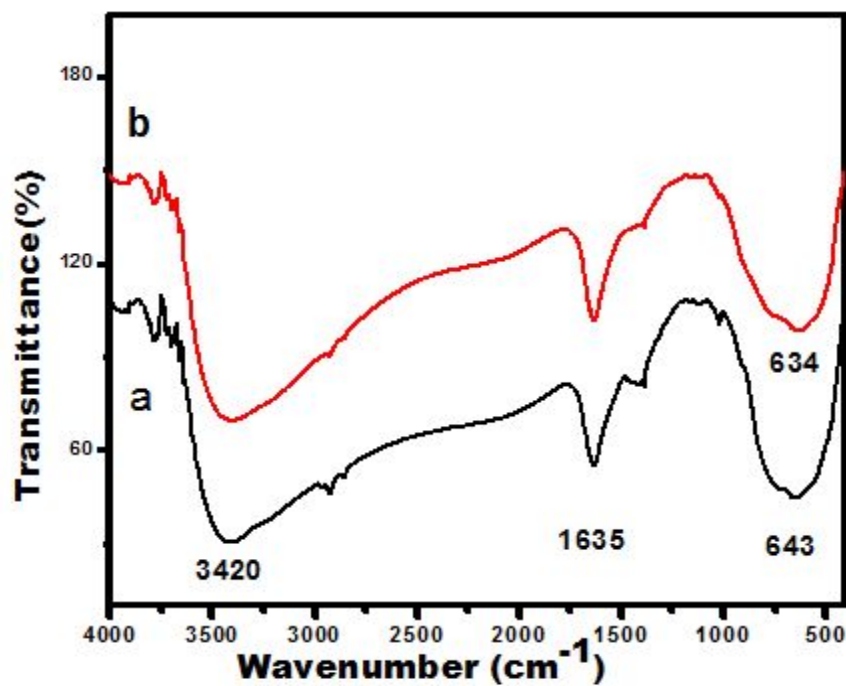


Figure 5 FTIR Spectrum of calcinated at 500°C a) Pure TiO_2 and b) Ni doped TiO_2

Temporal evolution of the spectral changes taking place during the photodegradation of Methylene blue mediated by typical Ni doped TiO_2 and pure TiO_2 (900°C for 1 hr) under solar light is displayed in figure 6. Methylene blue showed a major absorption band at 664 nm . The reduction in the intensity of the absorption band at 664 nm in turn suggests the reduction in the MB concentration. In the presence of Ni doped TiO_2 , MB is fully degraded within 30 min, while pure TiO_2 did not fully degraded MB at 30 min under solar light. Figure 7 shows visible Light Photocatalytic Mechanism. The formation of superoxide anion and hydroxide radical are clearly depicted in the figure. These identities are responsible for the decomposing of organic contaminants in the presence of photocatalyst and photons. The superoxide anion and hydroxide radical convert the organic dye into CO_2 and H_2O . Thus the concentration of the organic dye reduces with time in the presence of solar light and photocatalyst. A detailed mechanism involved in photocatalysis has been discussed in our earlier publication [22]

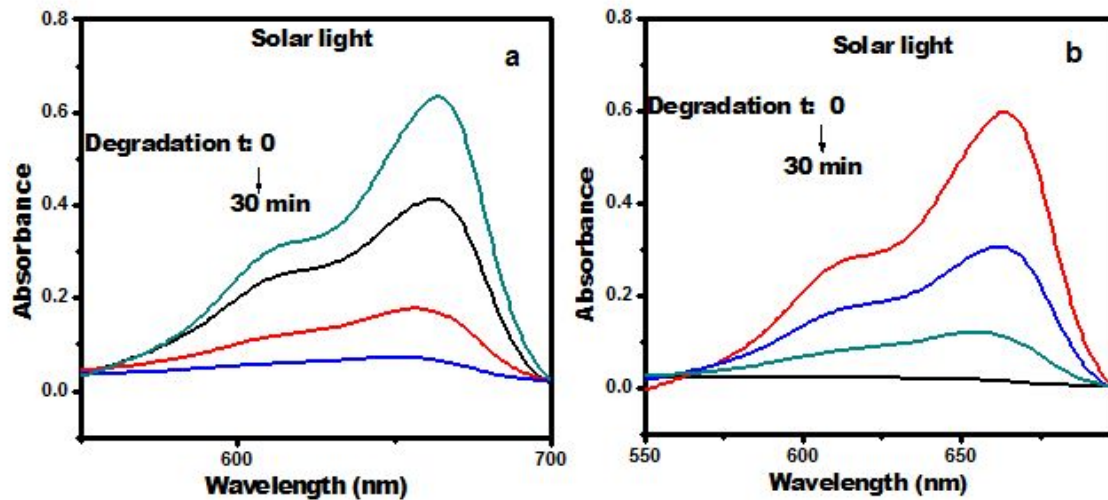


Figure 6 Photodegradation of Methylene blue a) pure TiO_2 calcinated at 900°C under solar light degradation b) Ni doped TiO_2 calcinated at 900°C under solar light degradation

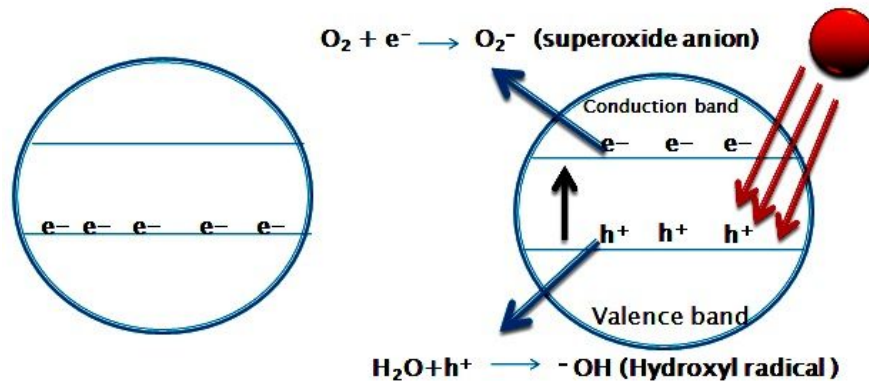


Figure 7 Photocatalytic Mechanism

4 Conclusion

The pure and Ni doped TiO_2 powders are successfully synthesized by novel Photon Induced Method. The effect of doping Ni on the properties of the prepared TiO_2 samples have been studied, compared and reported. XRD results reveal that doping Ni favours the rutile phase formation. Moreover, the HRTEM results reveal a formation of nanorod like structures on doping with Ni. However with increase in calcination temperature the crystallite size and particle size of pure TiO_2 increases whereas the Ni doped TiO_2 samples show a decreasing trend. The EDAX spectrum confirms the doping of Ni into TiO_2 matrix. The photocatalytic performance of the TiO_2 catalyst seen to get promoted on doping with Ni. The Ni doped TiO_2 samples degraded Methylene blue dye in the presence of sunlight within 30 min, thus the photocatalyst prepared by this novel method opens the gate for new research.

Acknowledgement

The authors would like to thank the management Sacred Heart College, Tirupattur for providing necessities facilities.

Reference

- [1] X.B chen, S.H.Shen, L.J. Guo, S.S. Mao. Chemical reviews 110, 6503-6507, 2010
- [2] M.G. Walter, E.L. Warren, J.R. Mckone, S.W.Boettcher, Q. Me, Chemical Reviews 110, 6446-6449, 2010
- [3] A. Hagfeldt, G. Boschloo, L.Sun, L. Kloo, H. Pettersson, Chemical Reviews 110, 6595-6599, 2010.
- [4] X.L. Cui, Z.Z. Li, Y.C. Yang, W. Zhang, Q.F. Wang, Electroanalysis 20, 970-974, 2008
- [5] W. Choi, A. Termin and M.R. Hoffmann. J.Phys.Chem.,98, 13369-13374, 1994
- [6] T. Morikawa, R. Asahi, T. Ohwaki, A. Aoki, and Y. Taga. Jpn. T. Appl. Phys.40, part 2, L561, 2001
- [7] H. E. Chao, Y. U. Yun, H. U. Xingfang, and A. Larbot.J. Eur. Ceram. Soc. 23,1457-64, 2003
- [8] Abbasi M., Asl N.R. Journal of Hazardous Material, 153, 942-947, 2008

- [9] Wang, X. Li, Z. Shi, J. Yu, Y. *Chem. Rev.* 114, 9346-9384, 2014
- [10] Bilik, P. and G. Plesch. *Mater. Lett.* 61,1183-1186, 2007
- [11] L.Znaidi, R.Seraphimov, J.F.Bocquet, *Mater.Res.Bull.* 36, 1-6, 2001
- [12] Ismail AA, Bahnemann DW. *Journal of Materials Chemistry.* 21,11686-11707, 2011
- [13] Tang H, Lévy F, Berger H, Schmid PE. *Physical Review B.* 52, 7771-7774, 1995
- [14] Dar MI, Chandiran AK, Grätzel M, Nazeeruddin MK, Shivashankar SA. *Journal of Materials Chemistry A.* 2, 1662-1667, 2014
- [15] D. Madare, M. Tasca, M. Delibas, and G. I. Rusu. *Appl.Surf. Sci.*,156, 200-2004, 2000
- [16] M.M. Rahman, K.M. Krishna, T. Soga, T. Jimbo, and M. Umeno.*J.Phys.Chem. Solids.* 60, 201-205, 1999
- [17] K.M. Krishna, M. Mosaddeq-ur-Rahman, T. Miki, T.Soga, K.Igarashi, S. Tanemura, and M. Umeno. *Appl.Surf.Sci.* 149, 113-115, 1997
- [18] L.-L. Tan, W.-J. Ong, S.-P. Chai, A.R. *Chem. Commun.* 50, 6923–6926, 2014
- [19] L-L. Tan, W.-J. Ong, S.-P. Chai, A.R. Mohamed. *Nanoscale Res. Lett.* 8, 465-468, 2013
- [20] V. Etacheri, M.K. Seery, S. J. Hinder, S. C. Pillai, *Adv. Funct. Mater.* 21, 3744-3752, 2011
- [21] D. Pei, J. Luan, *Int. J. Photoenergy.* 13, 2012
- [22] Prasetyo Hermawan, Harno Dwi Pranowo, and Indriana Kartini. *Indo. J. Chem.*,11, 135 – 139, 2011
- [23] Siti Nur Fadhilah Zainudin, Masturah Markom, and Huda Abdullah. *Advanced Materials Research.* 879,199-205, 2014
- [24] G. Nagaraj, A. Dhayal Raj, A. Albert Irudayaraj, *Materials science: Materials in Electronics.* 1-9, 2017
- [25] A. Dhayal Raj, P. Suresh Kumar, D. Mangalaraj, N. Ponpandian, A. Albert Irudayaraj, Q. Yang, *Sens. Lett.* 10, 825–831, 2012
- [26] N. Yang, J. Zhai, D. Wang, Y. Chen, L. Jiang. *ACS Nano* 4, 887–894, 2010
- [27] J. Shen, B. Yan, M. Shi, H. Ma, N. Li, M. Ye. *J Mater Chem* 21, 3415–3421, 2011
- [28] K. Zhou, Y. Zhu, X. Yang, X. Jiang, C. Li. *New J Chem* 35, 353–359, 2011
- [29] Z. Wang, B. Huang, Y. Dai, Y. Liu, X. Zhang, X. Qin, J. Wang, Z. Zheng, H Cheng. *Cryst Eng. Comm* 14, 1687–1692, 2012
- [30] L. Pan, JJ. Zou, S. Wang, XY. Liu, X. Zhang, L. Wang. *ACS Appl Mater Interfaces* 4, 1650–1655, 2012
- [31] J. Arumugam, A. Dhayal Raj, A. Albert Irudayaraj. *J Mater Sci: Mater Electron* 28, 3487-3494, 2017
- [32] W-S. Wang, D-H. Wang, W-G. Qu, L-Q. Lu, A-W. Xu. *J Phys Chem C* 116,19893–19901, 2012
- [33] MS. Sher Shah, AR. Park, K. Zhang, JH. Park, PJ. Yoo. *ACS Appl Mater Interfaces* 4, 3893–3901, 2012